Neurology®

Postganglionic sudomotor denervation in patients with multiple system atrophy

Vincenzo Provitera, Maria Nolano, Giuseppe Caporaso, et al.

This information is current as of May 16, 2014

The online version of this article, along with updated information and services, is located on the World Wide Web at:

http://www.neurology.org/content/early/2014/05/16/WNL.0000000000000518.full.html

AMERICAN ACADEMY OF NEUROLOGY®

Postganglionic sudomotor denervation in patients with multiple system atrophy

Vincenzo Provitera, MD*

Maria Nolano, MD*

Giuseppe Caporaso, BS

Annamaria Stancanelli, TN

Fiore Manganelli, MD

Rosa Iodice, MD

Mona M. Selim, MD

Anna De Rosa, MD

Bernardo Lanzillo, MD

Maria Teresa Pellecchia, MD

Giuseppe De Michele, MD

Lucio Santoro, MD

Correspondence to
Dr. Provitera:
vincenzo.provitera@fsm.it

ABSTRACT

Objective: To evaluate postganglionic autonomic involvement in multiple system atrophy (MSA).

Methods: We quantified sudomotor innervation in skin biopsy of 29 patients with MSA (19 male and 10 female; age 60.0 ± 7.7 years) and 29 age- and sex-matched healthy subjects. Samples were obtained from thigh and leg and, in 20 out of the 29 cases, also from fingertip. Dysautonomic complaints were evaluated by SCOPA-AUT, a self-administered questionnaire. Sudomotor function was evaluated in a subgroup of patients by the silastic imprint test. Skin samples were processed by indirect immunofluorescence using pan-neuronal and selective cholinergic markers. Total length of sudomotor nerves was measured on digital confocal images using a semiautomated morphometric approach.

Results: Measurements of sudomotor nerve density (total length of nerve per volume of glandular tissue) favorably correlated to values obtained using a stereologic unbiased method. Sudomotor nerve density was lower in patients compared to controls in all the examined sites (0.9 ± 0.2 vs 1.9 ± 0.4 nm/μm^3, $p < 0.001$, in fingertip; 0.7 ± 0.2 vs 1.9 ± 0.5 nm/μm^3, $p < 0.001$, in thigh; 0.6 ± 0.2 vs 1.8 ± 0.4 nm/μm^3, $p < 0.001$, in leg).

Conclusions: Our data support the hypothesis that postganglionic impairment occurs in MSA and may contribute with the coexisting degeneration of central structures to the development of dysautonomic disorders in this condition. *Neurology*® 2014;82:1–7

GLOSSARY

CollV = collagen IV; **ENF** = epidermal nerve fiber; **GDS-UMSARS** = global disability score of the Unified MSA Rating Scale; **ICC** = intraclass correlation coefficient; **MBFB** = Microbrightfield Bioscience; **MSA** = multiple system atrophy; **PD** = Parkinson disease; **PGP** = protein gene product; **SCOPA-AUT** = Scales for Outcomes in Parkinson's disease–Autonomic; **SIT** = silastic imprint test; **VIP** = vasoactive intestinal peptide.

Multiple system atrophy (MSA) is a neurodegenerative disease characterized by the progressive involvement of multiple neurologic domains. According to the most recent guidelines,[1] autonomic dysfunction is necessary for a premortem diagnosis. In addition to orthostatic hypotension and genitourinary dysfunction, sudomotor failure is a common finding.[2] Despite its clinical relevance, the anatomic sites responsible for dysautonomia in MSA remain disputed; although preganglionic involvement is considered the cause,[3] abnormalities of postganglionic sympathetic neurons have also been suggested.[4] Determining whether or not postganglionic neurons are involved in MSA is not a minor issue. Actually, postganglionic involvement in patients with early extrapyramidal symptoms is thought to help differentiate between Parkinson disease (PD) and MSA.[5] However, attempts aimed at confirming or disconfirming the involvement of postganglionic fibers in MSA have been inconclusive.[6,7]

Morphometric analysis of autonomic nerves residing in the skin is a promising investigative tool.[8] Cutaneous annexes are abundantly innervated by postganglionic sympathetic autonomic fibers.[9] These nerves are easily accessible through a minimally invasive punch biopsy.[10] Current

**Supplemental data
at Neurology.org**

imaging technology allows for high-resolution 3D digital images of cutaneous annexes that are suitable for morphometric evaluation.

We quantified sweat gland innervation in skin samples from patients with MSA and from healthy subjects in an attempt to assess the postganglionic portion of the sudomotor pathway. We utilized a new method of quantification with semiautomated tracking of nerve fibers through 3D images using a software that determines nerve trajectories in the x, y, and z planes and subsequently traces complex structures.[11] To validate this procedure, we compared the results with measurements from standard unbiased stereology.[12]

METHODS **Subjects.** Twenty-nine patients (19 men, 10 women; age 60.0 ± 7.7 years; disease duration 2.7 ± 1.3 years) were enrolled consecutively from 2006 to 2012 with probable (21 patients) or possible (8 patients) MSA, according to the second consensus statement on the diagnosis of MSA.[1] The phenotype was characterized by prevalently cerebellar features in 16 and by parkinsonian signs in the remaining 13 patients. Disease severity was evaluated using the global disability score of the Unified MSA Rating Scale[13] (GDS-UMSARS). Clinical involvement of autonomic domains was evaluated using the Scales for Outcomes in Parkinson's disease–Autonomic (SCOPA-AUT), a self-administered questionnaire developed to assess autonomic symptoms in patients with PD.[14] Recently this questionnaire has proved reliable for the screening of autonomic symptoms in MSA.[15] Patients' clinical evolution was followed between 2006 and 2012. Five out of 8 patients, classified at enrollment as possible MSA, at the end of follow-up fulfilled the criteria for probable MSA. Average GDS-UMSARS score was 2.6 ± 1.3 at baseline and 4.4 ± 1.0 at follow-up. Demographics along with clinical data are reported in table e-1 on the *Neurology*® Web site at Neurology.org.

At the time of enrollment, all subjects underwent clinical and electrophysiologic evaluation and performed skin biopsies from 3 body sites: proximal thigh, distal leg, and fingertip, except for 9 patients who opted out of the fingertip biopsy. Twenty-nine age- and sex-matched healthy subjects were also included in the study as controls for morphologic study. Age differences ≤2 years have been allowed in order to compose the case/control pairs. In 12 pairs out of 29, age differences were greater than 0.

At enrollment, patients also completed the SCOPA-AUT questionnaire to assess autonomic involvement. The questionnaire is composed of 23 items exploring the occurrence of symptoms related to the function of 6 different autonomic domains. For each item, the score ranges from 0 to 3. We assumed a domain was involved if at least 1 item obtained a score of 2.

Immunohistochemistry and image acquisition. Skin samples (3-mm punch) were fixed overnight in Zamboni solution (picric acid and paraformaldehyde) and then cryoprotected in 20% sucrose phosphate-buffered saline. Fifty-micrometer-thick sections were cut using a freezing sliding microtome (Leica 2000R; Nussloch, Germany) and labeled for indirect immunofluorescence according to a previously published procedure.[16]

Using a nonlaser confocal microscope (AxioImagerM2 with Apotome2; Zeiss, Göttingen, Germany), 3D digital images of sweat glands were acquired using a 20× objective (Zeiss EC Plan NeoFluar 20×/0.5). To avoid nonrepresentative sweat gland fragments, only sweat glands at least 25 μm thick were included in quantifications. A minimum of 4 sweat glands per site were identified and imaged: 2 marked with the marker for cholinergic fibers vasoactive intestinal peptide (VIP; SC25347, 1:300 dilution; Santa Cruz Biotechnology, Dallas, TX) and 2 with the pan-neural marker protein gene product 9.5 (PGP 9.5; E3344, 1:400 dilution; Biospring, Frankfurt am Main, Germany). For sweat gland volume quantification, imaging was acquired using markers for collagen IV (ColIV; MAB1910, 1:800 dilution; Chemicon, Billerica, MA) and Ulex Europaeus agglutinin I (B1065, 1:100 dilution; Vector, Burlingame, CA), in addition to the specific neural marker.

Quantification of sudomotor nerves. *Semiautomated morphometry.* Sudomotor nerve length density (nm/μm³) was calculated using the nerve tracing module Autoneuron, a part of Neurolucida software (Microbrightfield Bioscience [MBFB], Williston, VT). Briefly, within the 3D confocal image stack of nerve-associated immunoreactivity, nerve fibers were identified with a series of single voxels. The software identified the voxels with the highest probability of being nerve-associated. It then traced the nerve trajectory that was morphologically compatible with the antibody and within the specified parameters of x, y, and z planes (figure 1, A, B, D, and F). The software was set up to only trace continuous, linear structures at least 10 μm in length with a defined thickness (between 0.8 and 2.5 μm for PGP staining and between 0.8 and 2.0 μm for VIP staining). Such rules, based on the characteristics of nerve-associated staining, exclude non-nerve-related fluorescence from quantification. After completion of the 3D tracing, the total length was recorded and later converted to a length density after calculating the volume of the imaged gland (figure 1H). Sweat gland volume was calculated by manually tracing the outside contour on alternate optical sections of composite confocal images showing PGP 9.5, ColIV, and Ulex; this procedure ensured that no portions of the gland were accidently excluded due to denervated tubules. To verify the repeatability of the method, 2 investigators blinded to disease or control state quantified sudomotor innervation in 40 3D confocal images of sweat glands, 20 with each neural stain (VIP and PGP 9.5).

Unbiased stereology. To verify the accuracy of the semiautomated nerve tracing method, a group of 40 sweat glands were requantified by adopting unbiased stereology using the software StereoInvestigator (MBFB). Nerve length was estimated using the isotropic spherical probe,[17,18] which estimates total length by counting the intercepts between nerves and a virtual spherical probe systematically and randomly distributed at known distances within the tissue (figure 1, A, C and E). Sweat gland volume was estimated with the Cavalieri method (figure 1G).[19]

To compare autonomic and somatic involvement in patients, the linear density of epidermal nerve fibers (ENFs) was quantified in all skin samples using standard procedures.[10]

Functional evaluation. In a subgroup of 10 patients, a functional sudomotor evaluation was performed using the silastic imprint test[20] (SIT) to calculate the density of sweat glands activated by iontophoresis of 1% pilocarpine. Results were compared with laboratory age- and sex-stratified normative dataset.

Statistical analysis. Numerical data are presented as mean ± SD. We assessed the distribution of our data using the Shapiro-Wilk test. Since 4 out of 9 series of data were not normally distributed, we used the Mann-Whitney test to evaluate differences between control subjects and patients, and between

Figure 1   Methods used to quantify sudomotor innervation
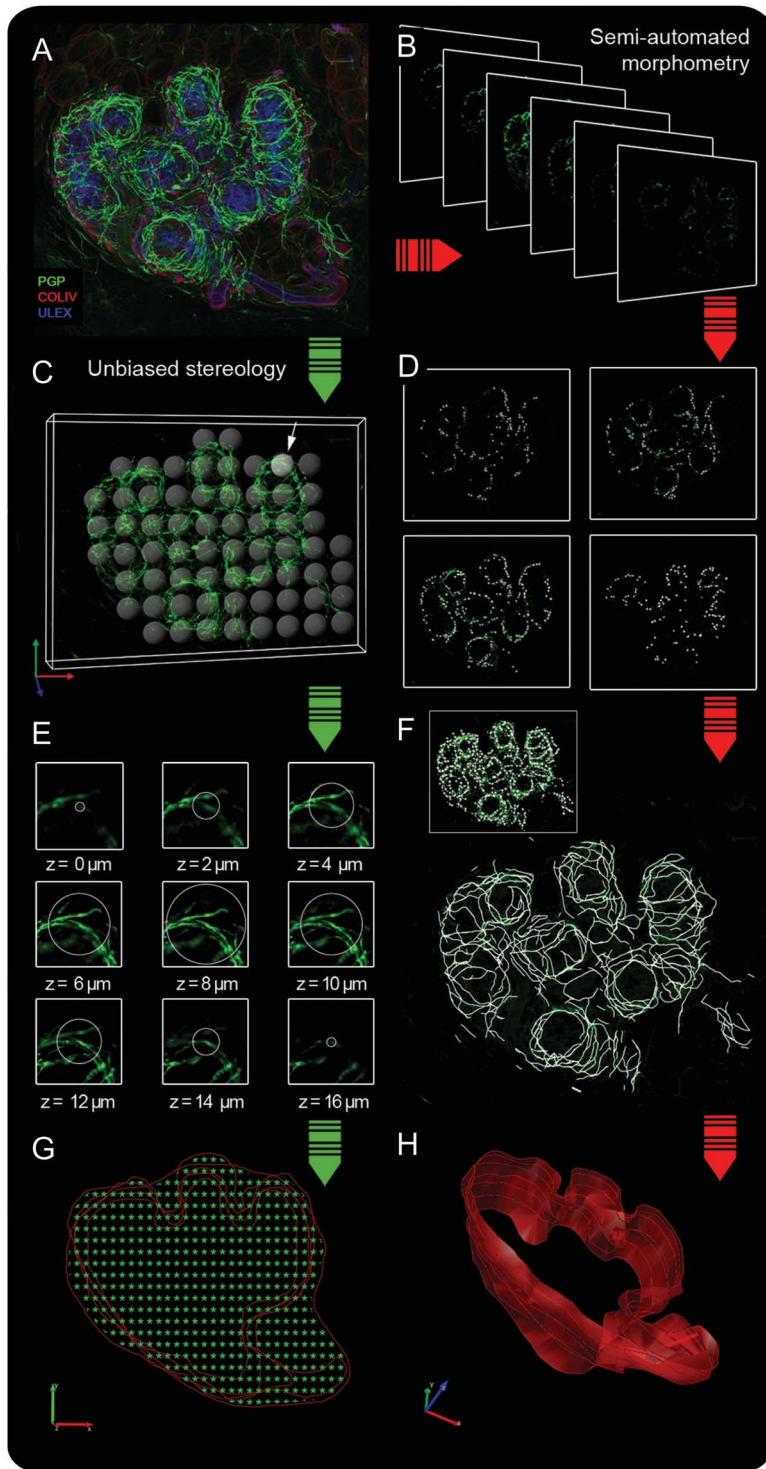
(A) Projection of a 3D triple-stained (protein gene product [PGP] 9.5, collagen IV [ColIV], and Ulex) confocal image of a sweat gland. Semiautomated method (red path): the software identifies within the z-series stack of nerve-associated immunoreactivity (B) the voxels with the highest probability of being nerve-associated (D). Then, starting from these voxels, the software traces the nerve trajectory (F) and measures its total length. The total length is reported as a length density (nm/μm^3) after calculating the volume of the imaged gland interpolated in 3D (H) by manually tracing its outside contour on the optical sections of the composite confocal image. Unbiased stereology method (green path): the software places virtual spherical probes systematically and randomly within the tissue (C). Then the operator selects all the intercepts between nerve fibers and the profile of the probe through the z-stack (E) before obtaining the unbiased estimation of total nerve length. The volume of the gland is calculated with the Cavalieri method (G).

patients with different phenotypes. Bonferroni correction for multiple testing was applied and a p value < 0.05 was considered significant.

Intraclass correlation coefficient (ICC) between measures performed on the same gland sample by different operators was used to assess interrater repeatability. Bland-Altman analysis was used to assess agreement between the 2 methods of sudomotor nerve quantification (semiautomated morphometry and unbiased stereology). Pearson regression was used to assess the correlation between morphologic data on one side and functional data, age, disease duration, autonomic involvement, and disease severity on the other side.

Standard protocol approvals, registrations, and patient consents. All participants signed a written informed consent and the study was approved by the institutional ethical committee.

RESULTS According to scores on the self-administered SCOPA-AUT questionnaire (table e-1), among different autonomic domains, the urinary was the more frequently (26 out of 29 patients) affected and the pupillomotor the less frequently (7 out of 29 patients) affected. The thermoregulatory domain was involved in 14 out of 29 patients. Average cumulative SCOPA-AUT score was 18.2 ± 3.8.

Morphologic data. Bland-Altman analysis (figure e-1) showed a mean difference between the 2 methods of nerve quantification greater than zero (0.39 nm/μm^3 with a SD of 0.74 nm/μm^3) but adequate to appreciate the differences that we observed between patients and controls. Moreover, semiautomated measures of sudomotor nerve density performed on the same subset of 40 glands by 2 operators showed a good repeatability of the procedure (ICC $= 0.9$, $p < 0.001$).

Using semiautomated morphometry, we quantified sudomotor innervation of 865 sweat glands: 420 from 29 patients with MSA (232 with PGP 9.5 and 188 with VIP) and 445 from 29 control subjects (243 with PGP 9.5 and 202 with VIP). Quantitative data are summarized in table 1.

Sudomotor nerve density was lower in MSA compared to control subjects ($p < 0.001$). This finding was evident at the thigh and distal leg using both the pan-neuronal marker PGP 9.5 and the specific cholinergic marker VIP (figure 2). At the fingertip, sudomotor nerve fiber loss was significant ($p < 0.001$) only with the cholinergic marker, whereas no statistical significance ($p = 0.7$) was attained using PGP 9.5. We found a non-length-dependent loss ($p < 0.05$) of ENFs in patients with MSA in all the examined sites compared to control subjects.

Sudomotor functional evaluation. SIT showed a reduction ($p < 0.05$) of the density of sweat glands activated by direct pharmacologic stimulation in patients with MSA (45.1 ± 24.3 sweat glands/cm^2) compared to controls (102.6 ± 19.8 sweat glands/cm^2), and the loss correlated ($p < 0.05$, $r = 0.56$) with sudomotor nerve fiber density at the distal leg.

Sudomotor nerve loss did not correlate ($p > 0.05$) with disease severity as expressed by the GDS-UMSARS, with clinical autonomic involvement, with age, or with disease duration, regardless of the site (thigh, leg, or fingertip) and the nerve marker (PGP or VIP). All patients, even those with less than a year disease duration, showed an abnormal sweat gland nerve fiber density in at least 2 of the 3 examined sites, with no difference between cerebellar and parkinsonian phenotypes ($p > 0.05$) or between patients with and without clinically appreciable thermoregulatory disturbances ($p > 0.05$). The loss observed at proximal and distal sites on the leg was comparable (about 60% loss compared to control values).

DISCUSSION This study demonstrates histologic involvement of postganglionic autonomic fibers in MSA by showing a reduced innervation of sweat glands. The degree of sudomotor denervation was comparable at proximal and distal sites of the lower limb, suggesting a ganglionopathy rather than a length-dependent neuropathic process. Autonomic nerve loss did not correlate with clinical impairment as assessed by the SCOPA-AUT questionnaire, nor were we able to demonstrate a more severe sudomotor denervation in patients with a clinical impairment of thermoregulation. We observed a correlation between sudomotor nerve loss and functional sudomotor impairment, however.

This is not the first attempt at quantifying nerves of dermal annexes, but the complexity of these structures makes accurate quantification a challenging task. Methods based on semiquantitative evaluations[21] or on the quantification of nerve-related fluorescence (based on the arbitrary selection of a brightness threshold)[22] seem unreliable as they are incapable of detecting small variations in nerve density. More accurate measurements, following validation with stereologic methods, have been successfully used to demonstrate sudomotor denervation in other pathologies.[8] We used a semiautomated method previously shown to be reliable and reproducible in the quantification of the complex mucosal nerves in patients with idiopathic chronic childhood constipation.[23]

The agreement between the results from our 2 independent operators was expected as, within a confocal image stack, nerve tracking is an automated process and outlining of a sweat gland is the only operator-dependent variable. We verified our results using stereology and found them to agree with length density estimates.

Quantification of a single sweat gland using the semiautomated method took approximately 10 minutes; this included optical field selection, acquiring digital images, and completing the nerve tracing. It was much more time-consuming (about 45 minutes)

Figure 2   Sudomotor innervation in multiple system atrophy and control
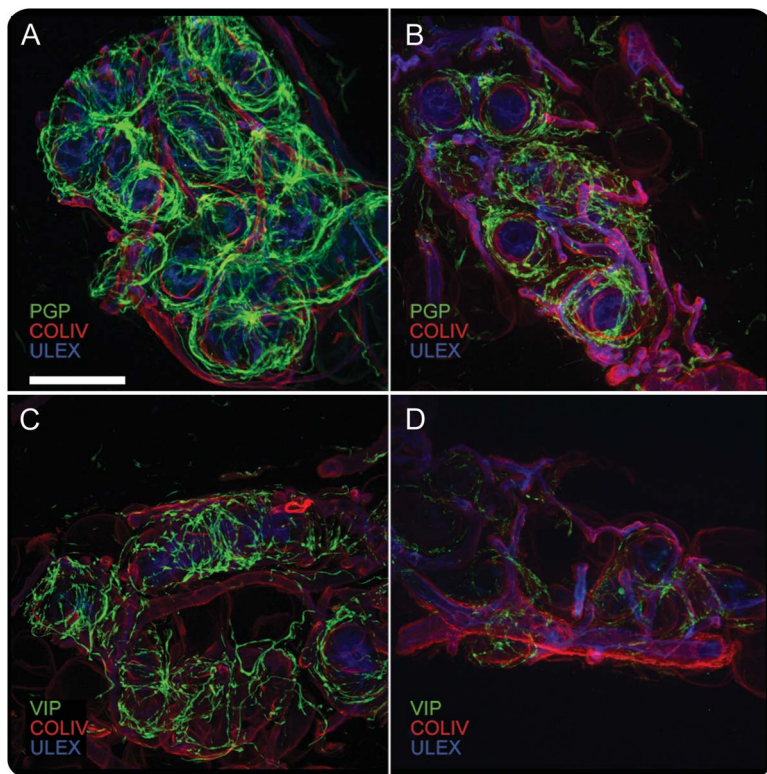
Confocal images of skin from a thigh show sweat gland innervation in a control subject (A, C) and a patient (B, D). The loss of sudomotor nerve fibers is evident using both the pan-neuronal marker protein gene product (PGP) 9.5 (B compared to A) and the selective cholinergic marker vasoactive intestinal peptide (D compared to C). 20× images. Scale bar is 100 μm. COLIV = collagen IV.

to complete the analysis of one sweat gland using stereology.

MSA is characterized pathologically by cell loss, gliosis, and glial cytoplasmic inclusions localized in several structures of CNS. Specifically, Lewy pathology and cell loss have been demonstrated in multiple autonomic nuclei such as the intermediolateral column of the spinal cord,[24] the ventrolateral portion of the intermediate reticular formation,[25] the dorsal motor nucleus of vagus,[26] ambiguus nucleus,[27] raphe nucleus,[28] arcuate nucleus,[29] and locus ceruleus.[30] Therefore, dysautonomia is usually considered secondary to the involvement of the preganglionic structures even though correlation between cell loss and the clinical degree of autonomic impairment is often unsatisfactory.[31]

It is assumed that sweating abnormalities in MSA are also preganglionic, resulting from the degeneration of central components of the sudomotor pathway.[5] The often-reported lack of postganglionic involvement mainly stems from comparisons to PD, where a more severe involvement of postganglionic sympathetic cardiac innervation, as evaluated by MIBG myocardic scintigraphy, is apparent.[32] Although relatively spared compared to PD, myocardic sympathetic innervation is impaired in patients with MSA when compared to healthy control subjects.[33]

MIBG scintigraphy was not included in the diagnostic protocol of our patients; therefore, we could not compare our data of cutaneous postganglionic denervation with the degree of adrenergic postganglionic cardiac denervation. However, our functional and morphologic findings are in agreement with other experimental data that suggest postganglionic involvement of the sudomotor pathway in MSA. In fact, an impairment of sudomotor postganglionic fibers has been demonstrated by a reduced sudomotor response after both direct[34] and axon reflex–mediated[35] pharmacologic stimulation. Moreover, postganglionic sympathetic denervation in MSA has been demonstrated in other structures such as the bladder internal sphincter,[36] and Lewy bodies spotted in sympathetic ganglia of patients with MSA[37] provide convincing pathologic evidence for the involvement of postganglionic sympathetic neurons.

We previously reported on peripheral nervous system involvement in diseases characterized mainly by CNS degeneration.[38] A few studies tried to demonstrate an impaired peripheral autonomic system in MSA by quantifying sudomotor nerves. These studies were inconclusive, possibly because of the relatively small number of subjects examined.[39] Recently, a loss of sudomotor nerves has been reported in skin biopsies from 3 out of 8 patients with MSA.[21] The authors suggest that the postganglionic impairment may be due to trans-synaptic cell death in patients with long-

standing disease. Our findings do not support this hypothesis. We found no correlation between sudomotor denervation and disease duration. Sudomotor denervation was present even in patients with less than 1 year of disease duration. Patients also demonstrated a coexisting, severe, generalized, and non-age-related ENF loss, for which a trans-synaptic degenerative mechanism is not plausible. Our findings suggest that the involvement of peripheral somatic and autonomic fibers may be part of the pathophysiology of MSA rather than a late secondary phenomenon.

Our MSA patient population displayed a sudomotor denervation that was evident at the lower limbs regardless of the neural marker used. At the fingertip, a more innervated and vascularized site, sweat glands displayed nerve fiber loss only with the specific cholinergic marker VIP. This finding supports previous observations of a loss of immunoreactivity that precedes the actual nerve loss in neurodegenerative processes.[40]

We demonstrated sudomotor postganglionic denervation in patients with MSA using a semiautomated quantitative method. The postganglionic involvement may be part of the disease, contributing with the coexisting degeneration of central structures to the development of the variety of autonomic symptoms depicted in MSA.

REFERENCES

1. Gilman S, Wenning GK, Low PA, et al. Second consensus statement on the diagnosis of multiple system atrophy. Neurology 2008;71:670–676.

2. Lipp A, Sandroni P, Low PA. Systemic postganglionic adrenergic studies do not distinguish Parkinson's disease from multiple system atrophy. J Neurol Sci 2009;281:15–19.

3. Iodice V, Lipp A, Ahlskog JE, et al. Autopsy confirmed multiple system atrophy cases: mayo experience and role of autonomic function tests. J Neurol Neurosurg Psychiatry 2012;83:453–459.

4. Ozawa T. Morphological substrate of autonomic failure and neurohormonal dysfunction in multiple system atrophy: impact on determining phenotype spectrum. Acta Neuropathol 2007;114:201–211.

5. Kimpinski K, Iodice V, Burton DD, et al. The role of autonomic testing in the differentiation of Parkinson's disease from multiple system atrophy. J Neurol Sci 2012;317:92–96.

6. Riley DE, Chelimsky TC. Autonomic nervous system testing may not distinguish multiple system atrophy from Parkinson's disease. J Neurol Neurosurg Psychiatry 2003;74:56–60.

7. Asahina M, Vichayanrat E, Low DA, Iodice V, Mathias CJ. Autonomic dysfunction in parkinsonian disorders: assessment and pathophysiology. J Neurol Neurosurg Psychiatry 2013;84:674–680.

8. Gibbons CH, Illigens BM, Wang N, Freeman R. Quantification of sweat gland innervation: a clinical-pathologic correlation. Neurology 2009;72:1479–1486.

9. Donadio V, Nolano M, Provitera V, et al. Skin sympathetic adrenergic innervation: an immunofluorescence confocal study. Ann Neurol 2006;59:376–381.

10. Lauria G, Hsieh ST, Johansson O, et al. Guideline on the use of skin biopsy in the diagnosis of small fiber neuropathy: report of a joint task force of the European Federation of Neurological Societies and the Peripheral Nerve Society. Eur J Neurol 2010;17:903–912.

11. Broser PJ, Erdogan S, Grinevich V, Osten P, Sakmann B, Wallace DJ. Automated axon length quantification for populations of labelled neurons. J Neurosci Methods 2003;169:43–54.

12. Kubínová L, Janáček J. Confocal microscopy and stereology: estimating volume, number, surface area and length by virtual test probes applied to three-dimensional images. Microsc Res Tech 2001;53:425–435.

13. Wenning GK, Tison F, Seppi K, et al. Development and validation of the Unified Multiple System Atrophy Rating Scale (UMSARS). Mov Disord 2004;19:1391–1402.

14. Visser M, Marinus J, Stiggelbout AM, Van Hilten JJ. Assessment of autonomic dysfunction in Parkinson's disease: the SCOPA-AUT. Mov Disord 2004;19:1306–1312.

15. Damon-Perrière N, Foubert-Samier A, De Cock VC, et al. Assessment of the SCOPA-AUT questionnaire in multiple system atrophy: relation to UMSARS scores and progression over time. Parkinsonism Relat Disord 2012;18:612–615.

16. Nolano M, Provitera V, Crisci C, et al. Small fibers involvement in Friedreich's ataxia. Ann Neurol 2001;50:17–25.

17. Nolano M, Provitera V, Caporaso G, et al. Cutaneous innervation of the human face as assessed by skin biopsy. J Anat 2013;222:161–169.

18. Mouton PR, Gokhale AM, Ward NL, West MJ. Stereological length estimation using spherical probes. J Microsc 2002;206:54–64.

19. Gundersen HJ, Jensen EB, Kiêu K, Nielsen J. The efficiency of systematic sampling in stereology: reconsidered. J Microsc 1999;193:199–211.

20. Kennedy WR, Navarro X. Sympathetic sudomotor function in diabetic neuropathy. Arch Neurol 1989;46:1182–1186.

21. Donadio V, Cortelli P, Elam M, et al. Autonomic innervation in multiple system atrophy and pure autonomic failure. J Neurol Neurosurg Psychiatry 2010;81:1327–1335.

22. Sommer C, Lindenlaub T, Zillikens D, Toyka KV, Naumann M. Selective loss of cholinergic sudomotor fibers causes anhidrosis in Ross syndrome. Ann Neurol 2002;52:247–250.

23. Wendelschafer-Crabb G, Neppalli V, Jessurun J, et al. Mucosal nerve deficiency in chronic childhood constipation: a postmigration defect? J Pediatr Surg 2009;44:773–782.

24. Benarroch EE, Smithson IL, Low PA, Parisi JE. Depletion of catecholaminergic neurons of the rostral ventrolateral medulla in multiple systems atrophy with autonomic failure. Ann Neurol 1998;43:156–163.

25. Benarroch EE, Schmeichel AM, Low PA, Parisi JE. Depletion of ventromedullary NK-1 receptor-immunoreactive neurons in multiple system atrophy. Brain 2003;126:2183–2190.

26. Benarroch EE, Schmeichel AM, Sandroni P, Low PA, Parisi JE. Involvement of vagal autonomic nuclei in multiple system atrophy and Lewy body disease. Neurology 2006;66:378–383.

27. Isozaki E, Matsubara S, Hayashida T, Oda M, Hirai S. Morphometric study of nucleus ambiguus in multiple system atrophy presenting with vocal cord abductor paralysis. Clin Neuropathol 2000;19:213–220.

28. Benarroch EE, Schmeichel AM, Low PA, Parisi JE. Involvement of medullary serotonergic groups in multiple system atrophy. Ann Neurol 2004;55:418–422.

29. Braak H, Rub U, Del Tredici K. Involvement of precerebellar nuclei in multiple system atrophy. Neuropathol Appl Neurobiol 2003;29:60–76.

30. Tohgi H, Tabuchi M, Tomonaga M, Izumiyama N. Selective loss of small myelinated and unmyelinated fibers in Shy-Drager syndrome. Acta Neuropathol 1982;57:282–286.

31. Daniel SE. The neuropathology and neurochemistry of multiple system atrophy. In: Mathias C, Bannister R, eds. Autonomic Failure: A Textbook of Clinical Disorders of the Autonomic Nervous System. Oxford: Oxford University Press; 1999:321–328.

32. Berding G, Schrader CH, Peschel T, et al. [N-methyl ^{11}C] meta-hydroxyephedrine positron emission tomography in Parkinson's disease and multiple system atrophy. Eur J Nucl Med Mol Imaging 2003;30:127–131.

33. Orimo S, Kanazawa T, Nakamura A, et al. Degeneration of cardiac sympathetic nerve can occur in multiple system atrophy. Acta Neuropathol 2007;113:81–86.

34. Baser SM, Meer J, Polinsky RJ, Hallett M. Sudomotor function in autonomic failure. Neurology 1991;41:1564–1566.

35. Cohen J, Low P, Fealey R, Sheps S, Jiang NS. Somatic and autonomic function in progressive autonomic failure and multiple system atrophy. Ann Neurol 1987;22:692–699.

36. Sakakibara R, Hattori T, Uchiyama T, Yamanishi T. Videourodynamic and sphincter motor unit potential analyses in Parkinson's disease and multiple system atrophy. J Neurol Neurosurg Psychiatry 2001;71:600–606.

37. Sone M, Yoshida M, Hashizume Y, Hishikawa N, Sobue G. alpha-Synuclein-immunoreactive structure formation is enhanced in sympathetic ganglia of patients with multiple system atrophy. Acta Neuropathol 2005;110:19–26.

38. Nolano M, Provitera V, Estraneo A, et al. Sensory deficit in Parkinson's disease: evidence of a cutaneous denervation. Brain 2008;131:1903–1911.

39. Donadio V, Nolano M, Elam M, et al. Anhidrosis in multiple system atrophy: a preganglionic sudomotor dysfunction? Mov Disord 2008;23:885–888.

40. Nolano M, Provitera V, Caporaso G, Stancanelli A, Vitale DF, Santoro L. Quantification of pilomotor nerves: a new tool to evaluate autonomic involvement in diabetes. Neurology 2010;75:1089–1097.

This information is current as of May 16, 2014

Updated Information & Services	including high resolution figures, can be found at: http://www.neurology.org/content/early/2014/05/16/WNL.00000 00000000518.full.html
Supplementary Material	Supplementary material can be found at: http://www.neurology.org/content/suppl/2014/05/16/WNL.00000 00000000518.DC1.html
Subspecialty Collections	This article, along with others on similar topics, appears in the following collection(s): **Autonomic diseases** http://www.neurology.org//cgi/collection/autonomic_diseases **Multiple system atrophy** http://www.neurology.org//cgi/collection/multiple_system_atrop hy
Permissions & Licensing	Information about reproducing this article in parts (figures,tables) or in its entirety can be found online at: http://www.neurology.org/misc/about.xhtml#permissions
Reprints	Information about ordering reprints can be found online: http://www.neurology.org/misc/addir.xhtml#reprintsus